Mine Water Environ (2010) 29:263–269
DOI 10.1007/s10230-010-0118-0

TECHNICAL ARTICLE

Dissolution Kinetics of Sulfate from Schwertmannite Under Variable pH Conditions

Susanta Paikaray · Stefan Peiffer

Received: 5 January 2010 / Accepted: 4 July 2010 / Published online: 23 July 2010

Abstract Sulfate mobilization was investigated under controlled laboratory conditions. Microbially synthesized schwertmannite (14.7 m^2/g specific surface area with 4.7 Fe:S molar ratio) was interacted at room temperature for 4 months with aqueous solutions between pH 5 and 8. More than 50% of the solid-phase sulfate was released during the initial 2 months and the rate was positively influenced by pH due to the competition of hydroxyl ions for SO_4^{2-}. More than 90% of the solid-phase sulfate was released within 4 months at pH 8. Infrared spectra demonstrate diminution and splitting of SO_4^{2-} adsorption bands, indicating possible structural changes within the solid phase as a result of SO_4^{2-} release. Transformation of schwertmannite to goethite was triggered by pH increase and was primarily responsible for the sulfate mobilization. Thus, schwertmannite that interacts with neutral to alkaline water can add significantly to the sulfate load of a stream.

Keywords Acidity generation · Acid mine drainage · Dissolution kinetics · FTIR · Pyrite oxidation · Schwertmannite, schwertmannite transformation, sulfate pollution

Introduction

High sulfate concentrations in ground and surface waters caused by acid rock drainage (ARD) are causing increased concern. Sulfate concentrations exceeding the drinking water permissible limits of 250 mg/L (Calabrese et al. 1989) have been reported from most mined areas in the world, and are a challenge for remediation (Nyamadzawo et al. 2007). Sulfide minerals (Eq. 1) in coal-mining districts and massive sulfide mines are oxidized upon interaction with ground or rain water, atmospheric oxygen, and/or bacterial activities (Valente and Gomes 2009). In addition to SO_4^{2-}, high concentrations of Fe(III) are also released, which can itself oxidize pyrite, or be removed from the aqueous phase as ferric hydroxy-sulfates (Toran 1987).

$$\begin{aligned}&\text{Fe-sulfides}(FeS_2, ZnS, PbS, Fe_{1-x}S) + O_2 + H_2O \rightarrow \\ &\quad \text{Fe-oxyhydroxides} + \text{Fe-oxyhydroxysulfates} + H^+ \\ &\quad + SO_4^{2-} + Fe^{2+}\end{aligned} \quad (1)$$

Schwertmannite ($Fe_8O_8(OH)_x(SO_4)_y$, $x = 8 - 2y$, $1 < y < 1.75$) is an iron oxyhydroxy sulfate mineral that commonly forms from ARD; it contains ≈15 wt% SO_4^{2-} and ≈40 wt% Fe (Bigham et al. 1990). Bigham et al. (1990) estimated that approximately 35% of the SO_4^{2-} is surface-adsorbed and can be easily desorbed by metal ion or anion exchange from mine waters or by transformation of the mineral to iron oxyhydroxides. Association of schwertmannite with goethite, hematite, and ferrihydrite in mine waters or complete transformation to the most stable end members releases significant proportions of SO_4^{2-} back to the aqueous phase (Eq. 2, Murad and Rojik 2003).

$$Fe_8O_8(OH)_x(SO_4)_y + 2xH_2O \rightarrow 8FeOOH + ySO_4^{2-} + 2xH^+ \quad (2)$$

Jönsson et al. (2005) conducted a schwertmannite aging experiment and found that ≈1,200 μmol/g SO_4^{2-} were released within 24 h at pH 9. Recent studies on schwertmannite stability in mine waters demonstrate SO_4^{2-} release upon formation of iron oxides at elevated pH (Jönsson et al. 2005; Schwertmann and Carlson 2005)

S. Paikaray (✉) · S. Peiffer
Deptartment of Hydrology, University of Bayreuth,
95440 Bayreuth, Germany
e-mail: susanta@uni-bayreuth.de

through mixing of mine effluent with stream waters. However, the kinetic controls of sulfate release have not been carefully addressed. The aim of the present study was to investigate the behavior of sulfate in the course of long-term exposure of schwertmannite to aqueous solutions at elevated pH.

Materials and Methods

Sampling

Schwertmannite samples were obtained from a mine water treatment plant that produces microbially-mediated schwertmannite within a pH range of 2.9–3.2 (Glombitza et al. 2007). The brownish-yellow precipitates were air dried at room temperature (22–25°C) after sampling. Sample fractions of <73 μm were separated by sieving and used for all analytical purposes. X-ray diffraction (XRD) analysis showed a partially-amorphous structure similar to the schwertmannites reported by previous researchers (Bigham et al. 1990; Schwertmann and Carlson 2005). Sulfate and iron concentrations in the solid phase were measured after dissolution in 6.0 N·HCl for 48 h (Winland et al. 1991).

Long Term Stability Experiments

Stability experiments were carried out for 4 months using 5 g/L (equivalent to 7.75 mmol/L SO_4^{2-}) sediment load in milli-Q water using polypropylene reactor vials with regular shaking (4–5 times per day) at room temperature and atmospheric pressure. The system was investigated at four different pH conditions, i.e., 5.0, 6.0, 7.0, and 8.0. The pH adjustments were done with NaOH/HCl prior to addition of schwertmannite samples. Due to release of protons during the aging processes (Eq. 2), additional pH adjustments were done daily using 1.0 N NaOH, and the amount of NaOH consumed was noted. Samples were collected at regular intervals for 4 months. Similar stabilization experiments were conducted at pH 3.0, i.e., within the stability range of schwertmannite (pH 3–4.5) to distinguish the role of higher pH on the fate of sulfate. The solid phase was separated by filtration and oven dried at 60°C.

Analytical Methods

Schwertmannite samples were characterized by X-ray diffraction (XRD, D5000, Siemens, Germany) and Fourier Transform Infrared (FTIR, Vector 22, Bruker Optik GmbH, Ettingen, Germany) methods. The samples were X-rayed using Co-Kα radiation (40 kV, 40 mA) from 2° to 80° 2θ and the X-ray difractograms were interpreted with the library evaluation program DiffracAT v. 3.3 or by comparing the *d*-values with reference spectra from previous studies. The FTIR spectra of the samples were studied using OPUS-NT software. 2 mg of the samples were mixed with 200 mg of KBr to make pellets, which were subjected to infrared radiation between 350 and 4,500 cm^{-1} wave number with 1 cm^{-1} resolution. 32 scans were collected for each measurement in transmission mode and the background spectra were subtracted automatically by background scans.

The aqueous phase was analyzed for Fe, SO_4^{2-}, and pH. Iron measurements were done spectrophotometrically (Cary 1E, Varian Analytical Instruments, Varian GmbH, Darmstadt, Germany) at 512 nm wavelength by the 1, 10-phenanthrolene method (Tamura et al. 1974). Fe(III) was calculated by difference in concentrations between $Fe_{(T)}$ and Fe(II). SO_4^{2-} concentrations were measured spectrophotometrically by the $BaCl_2$-Gelatin turbidimetry method at 420 nm (Tabatabai 1974). The pH measurements were made with a Mettler Toledo Inlab 412 electrode, precalibrated with pH 4.0 and 7.0 buffers.

Results

Characterization of Schwertmannite

Eight peaks at 0.146, 0.152, 0.168, 0.193, 0.230, 0.258, 0.330, and 0.545 nm *d*-spacing were observed from the XRD study (Fig. 1), consistent with previous observations of synthetic and natural specimens (e.g., Bigham et al. 1990). The broadening of the peaks demonstrates poor crystallinity, with the highest intensity peak at 0.258 nm. The infrared spectrum has absorption bands at 420, 610, 700, 840, 980, 1,120, 1,430, 1,630, and 1,730 cm^{-1}, which is typical of schwertmannite, corresponding to absorption of SO_4^{2-}, OH^-, and Fe–O groups. The elemental analysis yielded a Fe:S molar ratio of 4.7, with total iron (Fe^{2+} + Fe^{3+}) and SO_4^{2-} concentrations of 7.35 and 1.55 mmol/g, respectively (Table 1). The Fe:S molar ratio is comparable

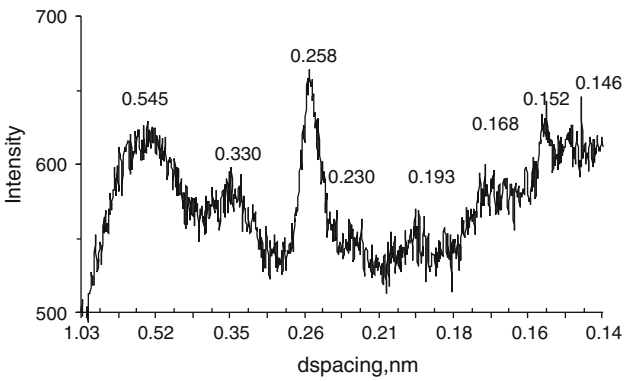

Fig. 1 X-ray diffractogram (XRD) of schwertmannite

Table 1 Characteristics of schwertmannite

$Fe_{(T)}$, mg/g	SO_4^{2-}, mg/g	Fe/S ratio	SSA (m^2/g)	Chemical formula	Major XRD bands (*d*, nm)	Major FTIR bands (wave #, cm^{-1})
410.8	148.6	4.7	14.7	$Fe_8O_8(OH)_{6.32}(SO_4)_{1.68}$	0.146, 0.152, 0.168, 0.193, 0.230, 0.258, 0.330, 0.545	420, 610, 700, 881, 1,050, 1,120, 1,430, 1,630, 1,730

to that of reported values (4.5–8) (Bigham et al. 1990; Childs et al. 1998), yielding the chemical formula as $Fe_8O_8(OH)_{6.32}(SO_4)_{1.68}$.

Sulfate Release as a Function of Time

Sulfate release was very rapid at all pH values; approximately 1.7–2.0 mmol/L were released during the initial 2 h of exposure. Steady release was observed for approximately 30 days, after which the rate of release decreased significantly (Fig. 2). A slow release of sulfate continued until 75 days, followed by a steady state with no major increase in aqueous phase sulfate concentrations until the end of the 120 day experiment. Sulfate concentrations exceeded the maximum permissible limits, i.e., 250 mg/L, within 30 days, 2 days, 12 h, and 10 h of exposure at pH 5, 6, 7, and 8, respectively. However, at pH 3, sulfate concentrations never exceeded 125 mg/L, even after 4 months. The total sulfate release after 4 months of exposure corresponded to 44.75 ± 0.44%, 56.86 ± 0.07%, 67.46 ± 1.33%, and 90.25 ± 0.56% of total solid phase sulfate at pH 5, 6, 7, and 8, respectively.

Sulfate Release as a Function of pH

The initial release of SO_4^{2-} was similar at all pH values, with 1.7–2.0 mmol/L SO_4^{2-} released within 2 h. However, the release rate increased with pH, especially as the pH was increased from 5 to 8 (Fig. 2). At pH 5, >250 mg/L sulfate was found after 30 days, while similar concentrations were observed after only 10 h at pH 8. Therefore, the highest concentration of sulfate release was found at pH 8 after 4 months of aging, corresponding to ≈90% of the initial solid-phase sulfate.

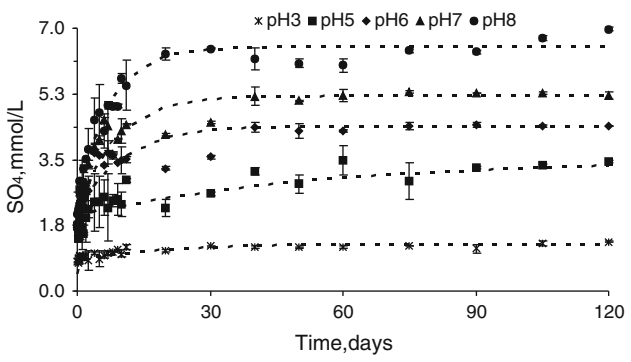

Fig. 2 Model predicated (lines) and experimental observations (points) of sulfate release rates with time at different pH within 120 days of schwertmannite stability

Sulfate Release due to Product Formation

Schwertmannite is metastable with respect to goethite at higher pH conditions (Bigham et al. 1990; Jönsson et al. 2005), and the transformation of schwertmannite to goethite releases significant amounts of SO_4^{2-} (Eq. 2). The X-ray difractograms for the aged products after 120 days are shown in Fig. 3. No significant changes in the diffractogram pattern were noted at pH 5 and 6, whereas

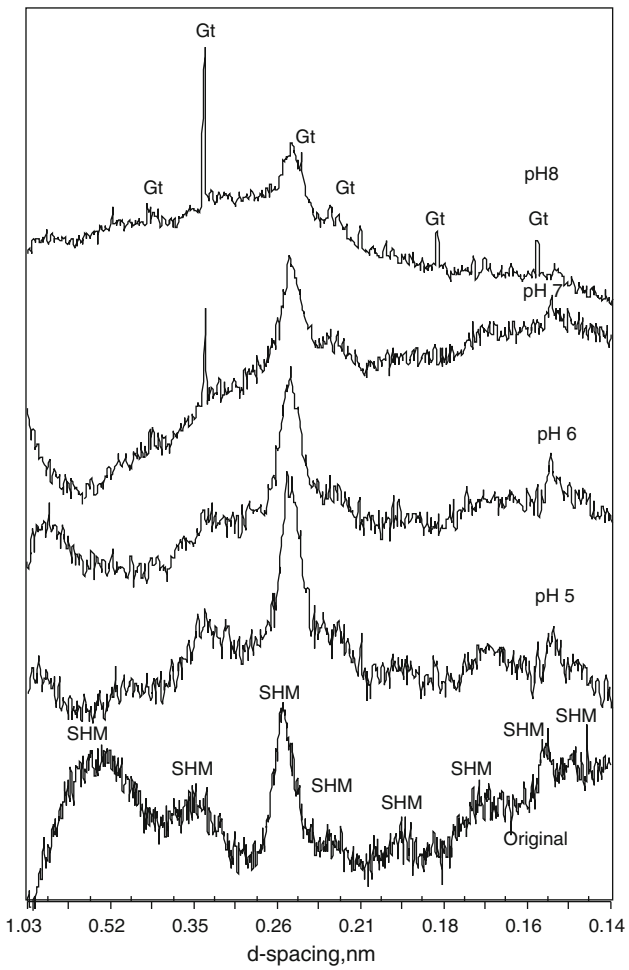

Fig. 3 X-ray diffractograms of aging products after 120 days at pH 5, 6, 7, and 8, compared to the original diffractogram (original)

formation of goethite can be observed at pH 7 and 8. This indicates that the transformation of schwertmannite with time is strongly pH-dependent.

The IR spectra obtained for the starting material and for selected aged specimens at different pH values are shown in Fig. 4. The three sulfate absorption bands are characteristic of schwertmannite (Bigham et al. 1990). The single broad band at 1,120 cm^{-1} is due to $v_3(SO_4)$ absorption, while that at 981 cm^{-1} is assigned to $v_1(SO_4)$; both bands correspond to outer-sphere sulfate (Regenspurg and Peiffer 2002). The absorption bands due to $v_4(SO_4)$ are located at 610 cm^{-1} and correspond to structural sulfate located in the tunnel cavities of the crystal. The bands at 420 cm^{-1} and 700 cm^{-1} are assigned to Fe–O stretching. The broad band at 1,630 cm^{-1} is due to the stretching and bending vibrations of protons in hydroxyls or water molecules. The COO^- band at 1,430 cm^{-1} is probably from organic impurities during synthesis.

The spectral patterns gradually changed during aging (Fig. 4), with eight distinct absorption bands at pH 5 resembling the original specimen. No major changes in absorption bands could be observed for pH 5 until day 120

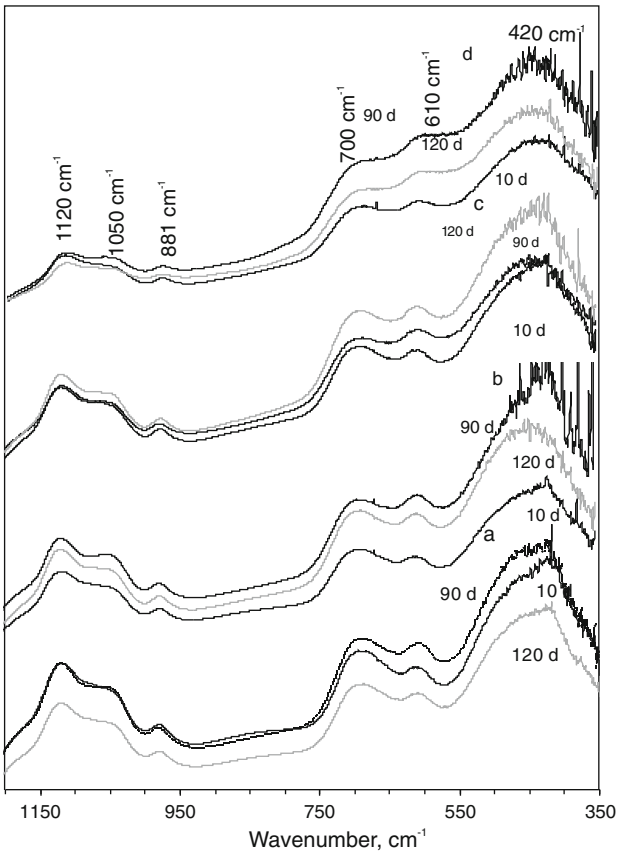

Fig. 4 Infrared absorption spectra for specimens after 10, 90 and 120 days at pH 5 (**a**), pH 6 (**b**), pH 7 (**c**) and pH 8 (**d**); note the absorption band patterns at 610 cm^{-1} and 1,120–1,050 cm^{-1}

except that the $v_4(SO_4)$ bands at 610 cm^{-1} showed a decrease in intensity. The decrease in the $v_4(SO_4)$ absorption band was more pronounced at higher pH and the intensity became negligible at pH 8 after almost 35 days. The $v_3(SO_4)$ absorption band, which corresponds to 1,050 cm^{-1} and 1,130 cm^{-1}, started to split and the 1,050 cm^{-1} peak became distinct after 75 day of aging at pH 5. The intensity of the 1,050 cm^{-1} absorption band increased at all pH values at the same time that the $v_4(SO_4)$ absorption band at 610 cm^{-1} decreased (Fig. 4). The intensity of the 1,050 cm^{-1} peak increased with time and the splitting of the $v_3(SO_4)$ absorption band became more pronounced at higher pH values.

Discussion

Sulfate Release as a Function of Time

Sulfate release took place in two steps: a very rapid release within hours, which is probably a desorption step based on reaction with pure water (Fig. 2), followed by a slow release until steady state was reached after about 30–50 days. The initial rapid release corresponded to ≥25% of the total sulfate. There was a negligible difference in the rate of sulfate release during this first step in the pH range 5–8, although differences were noted compared to pH 3.

To understand the behavior of SO_4^{2-} release as a function of time and pH, the reaction was modeled with the nonlinear statistical model Costat (version 6.002), using the kinetic approach (Eq. 3):

$$c = c_{eq}(1 - e^{-kt}) \quad (3)$$

where: c_{eq} = new equilibrium value after ≈50–120 days; c = calculated SO_4^{2-} concentration at any given time, t, and; k = rate constant. Kinetic constants were obtained from a linear plot of the expression:

$$\ln(c_{lev} - (c_i - c_{des})) \text{ vs. time} \quad (4)$$

where: c_{lev} = measured constant concentration at steady state; c_{des} = concentration of sulfate desorbed after 2–6 h, and; c_i = measured sulfate concentration after time step i. Both the percentage of sulfate released from the pool of sulfate remaining after the first desorption step and the kinetic rate constant show distinct pH dependence (Fig. 5). This indicates: (1) a decrease in solubility of the new phase, which drives the transformation rates, (2) that SO_4^{2-} release rates would be different in a system where desorbed SO_4^{2-} is being replaced by fresh contact media (here, mili-Q H_2O), and (3) the dissolution rate is strongly pH dependent, and is very much enhanced at low SO_4^{2-} concentrations.

Sulfate within schwertmannite is both structurally-bound and adsorbed to the surface (Bigham et al. 1990; Childs et al.

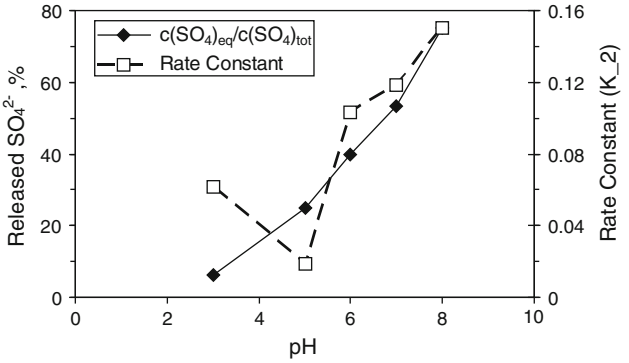

Fig. 5 Relationship between pH and SO_4^{2-} release (solid lines with filled symbols) and pH and rate constants K_2 (dashed lines with open symbols)

1998). Bigham et al. (1990) reported that 35% of the total SO_4^{2-} is adsorbed on the schwertmannite surface. Similar observations were reported by Jönsson et al. (2005), who found that 33% of the total SO_4^{2-} is adsorbed on the surface. The above kinetic results indicate that the rapidly released fraction was probably surface-adsorbed SO_4^{2-}, whereas the later release might be structural SO_4^{2-}.

Sulfate Release as a Function of pH

The direct relationship observed between sulfate release and pH suggests a dependence on aqueous hydroxyl ion concentration (Table 2). Stumm and Morgan (1996) demonstrated that as solution pH increases, surfaces of Fe-oxyhydroxides become less positively charged, and are therefore less favorable for SO_4^{2-} retention. The direct exchange of OH^- for SO_4^{2-} ion is possibly responsible for SO_4^{2-} desorption at higher pH conditions (Johnson and Cole 1977; Rose and Elliot 2000). A similar observation of 33–50% sulfate release was reported by Rose and Ghazi (1997) from amorphous sulfate-bearing iron oxyhydroxides at neutral pH in the course of treatment of mine precipitates by neutralizing materials.

Table 2 The relationship between pH and SO_4^{2-} release over time (in days) was graphed as a regression equation for straight line ($y = mx + c$), where 'y' denotes the amount of SO_4^{2-} released at any given time as a function of pH (x)

Time	Regression constants	Regression coefficient (R^2)
2	$m = 9.4$; $c = -7.8$	0.95
30	$m = 22.8$; $c = -67.0$	0.97
60	$m = 16.3$; $c = -14.8$	1.00
90	$m = 19.4$; $c = -33.1$	1.00
120	$m = 21.9$; $c = -45.8$	0.97

The constants in column 2 are the slope (m) and intercept (c) values of the regression equation. The key component is the relatively high R^2 values

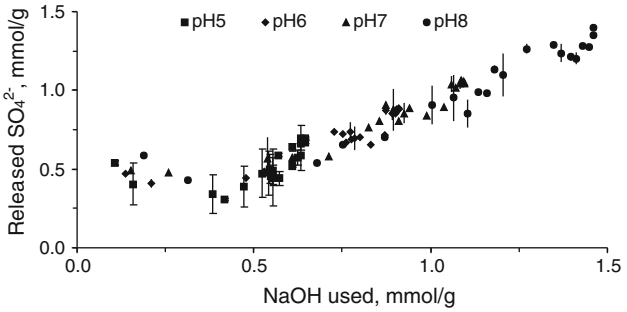

Fig. 6 Relationship between the amount of NaOH consumed and SO_4^{2-} release

The amount of OH^- consumed and SO_4^{2-} released were positively correlated (Fig. 6). This observation further illustrates the pH dependence of SO_4^{2-} release.

Sulfate adsorption onto hydrous ferric oxide (HFO) was modeled using PHREEQC 2.15.06 (Parkhurst and Appelo 1999), and the results were compared to the observed experimental data. HFO data were used because HFO is structurally similar to schwertmannite and because thermodynamic data for schwertmannite are still not available in the PHREEQC data base. Solutions equivalent to 8 mmol/L molar mass of schwertmannite were reacted with HFO with 300 m^3/g surface area. The percent of SO_4^{2-} adsorbed (adsorbed SO_4^{2-} at a given pH/adsorbed SO_4^{2-} at pH 3) and the model predictions are shown in Fig. 7. The SO_4^{2-} adsorption after 120 days of aging at pH 5 and 6 shows higher desorption, possibly due to high contributions from surface adsorbed SO_4^{2-}, while at elevated pH values, the experimental results were well matched with the model predictions, within an experimental error of 5%.

Sulfate Release due to Product Formation

From Fig. 3, it can be seen that schwertmannite is transformed to goethite at higher pH. Previous studies demonstrated the lower retention of anions, e.g., SO_4^{2-}, by more

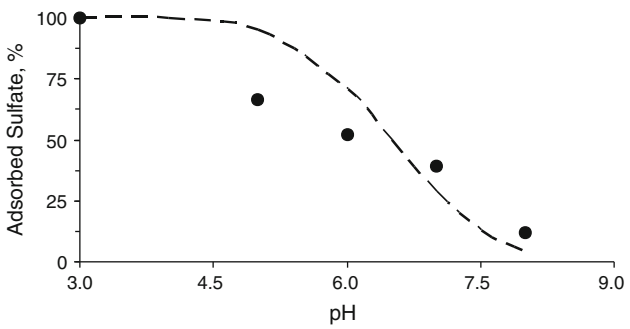

Fig. 7 PHREEQC modeled (lines) SO_4^{2-} adsorption profile by schwertmannite at different pH values. The experimentally observed values at pH 5, 6, 7, and 8 after 120 days are shown as filled circles

crystallized minerals (Houben 2003). Thus, surfaces of schwertmannite and aging products become unfavorable for SO_4^{2-} retention. Therefore, an increase in crystallinity due to transformation of schwertmannite to goethite could cause a release of excessive SO_4^{2-} into the aqueous phase. Due to higher crystallinity at pH 8, release of SO_4^{2-} would be comparatively greater.

Changes in sulfate absorption bands with respect to higher pH and time were observed (Fig. 4). The decrease in the intensity of the 610 cm^{-1} absorption band with increased pH and time suggests the disappearance of structural sulfate. Further, the splitting of the $v_4(SO_4^{2-})$ absorption band at 1,120 cm^{-1} and 1,050 cm^{-1} by an increase at 1,050 cm^{-1}, with a simultaneous decrease in the 1,120 cm^{-1} peak, suggests structural rearrangement. Sulfate desorption at pH 5 is minor, compared to other pH conditions, and the 610 cm^{-1} peak exists even after 120 days of aging. On the other hand, as pH was increased, the 610 cm^{-1} peak diminishes and after 30 days at pH 8, virtually all the surface-adsorbed sulfate was released. The absence of any significant IR band of goethite is presumably due to its low relative abundance in the sample.

The reaction kinetics clearly indicates the occurrence of two sulfate pools. The first can be attributed to adsorbed sulfate, which makes up $\approx$25% of the total sulfate. The second pool seems to be related to transformation of schwertmannite, where two processes are occurring: (1) transformation of schwertmannite to goethite, possibly via intermediate product formations, which is accompanied by a release of OH^- and (2) re-adsorption of sulfate to the new phase.

Implications for Mine Drainage Studies

In many ARD areas, ochre precipitates such as schwertmannite retain heavy metals from mine waters, but the same ochres can cause problems when hydrogeochemical conditions change. While caution must be taken in applying the results of our experimental study to field settings, where the interplay of ions and heavy metals can influence sulfate desorption behavior. This study indicates that increasing pH to neutral values (e.g., during ARD neutralization) can release more than 75% of the initial solid-phase sulfate, potentially causing a significant increase in the aqueous sulfate load (e.g., Kohfahl and Pekdeger 2004). For example, voluminous mine tailings associated with mines that had been abandoned decades ago have generated elevated concentrations of Fe ($\approx$200 ppm), Mn (3 ppm), Zn (7 ppm), and other contaminants in acidic lakes of the Lusatian lignite mines in eastern Germany, though the concentrations are much reduced (Fe = 7 ppm; Mn = 1.3 ppm, and Zn = 0.03 ppm) when the water becomes alkaline and the lake bottom sediments are consequently enriched (Friese et al. 1998). Sulfate is the major anion released from these mine tailings but much of the sulfate is precipitated as iron oxyhydroxide sulfate minerals (e.g., schwertmannite) or are sorbed onto iron oxyhydroxide surfaces. The solid phase SO_4^{2-} behavior strongly depends on the bonding type (strong bidentate bridging or weak surface adsorption through electrostatic attractions) which, as a consequence, influences differential release into the aqueous phase.

The pH has been observed to be the controlling factor for high SO_4^{2-} enrichment in ARD-affected environments. In our study, we found that duration of exposure is also very important in determining the extent and release of contamination. Schwertmannite exposed to neutral to alkaline pH released >50% of solid-phase SO_4^{2-} in few hours or a couple of days, depending on the pH. Thus, this reservoir of schwertmannite in the affected soils can ultimately control the overall SO_4^{2-} loading. Because of continuous precipitation of schwertmannite due to catalytic microbial activities in the ARD, the magnitude and intensity of SO_4^{2-} contamination is often unpredictable and likely to be higher at times than experimentally predicted. Aqueous SO_4^{2-} enrichment will continue until the sulfate reservoir is exhausted, either by mine water neutralizing processes (Rose and Elliot 2000) or by cyclic fluxes of surface water (Johnson and Cole 1977). Another implication of this current study is that additional acidity is generated by schwertmannite dissolution and/or transformation (Eq. 2). Overall, schwertmannite can be looked at as a SO_4^{2-} buffer in ARD environments, but the kinetics of sulfate release depends on both the pH and the aqueous SO_4^{2-} concentrations. These considerations imply that periods of high flow may not necessarily dilute sulfate concentrations, since the dissolution of schwertmannite that had precipitated during low flow conditions may be accelerated. Therefore, schwertmannite dissolution in mining districts has the potential to remarkably influence mine water geochemistry with respect to SO_4^{2-} levels and to generate additional acidity.

Conclusions

Long term exposure of schwertmannite to pH values between 5 and 8 for 4 months at normal atmospheric condition leads to high sulfate release into the aqueous phase, exceeding maximum drinking water permissible limits. Sulfate release increased with time and pH, up to roughly 1.40 mmol/g solid phase, corresponding to 90% of the total initial sulfate after 4 months of exposure at pH 8. The higher SO_4^{2-} release at elevated pH is probably due to the direct exchange of OH^- for the SO_4^{2-} ion at the schwertmannite surface, while the initially faster SO_4^{2-}

release may be due to the release of surface-adsorbed SO_4^{2-}. This study demonstrates that exposure of schwertmannite to neutral to alkaline pH stream waters for a long period could release more than 100 kg of SO_4^{2-} per 1 ton of schwertmannite in the mine area after 4 months of exposure.

Acknowledgments The work was supported by the German Academic Exchange Service (DAAD) and the Geotechnologien program (BMBF, No-03G0714A).

References

Bigham JM, Schwertmann U, Carlson L, Murad E (1990) A poorly crystallized oxyhydroxysulfate of iron formed by bacterial oxidation of Fe(II) in acid mine waters. Geochim Cosmochim Acta 54:2743–2758

Calabrese EJ, Gilbert CE, Pastides H (1989) Safe drinking water act: amendments, regulations, and standards. Lewis Publ, Chelsea, p 218

Childs CW, Inoue K, Mizota C (1998) Natural and anthropogenic schwertmannites from Towada-Hachimantai National Park, Honshu, Japan. Chem Geol 144:81–86

Friese K, Hupfer M, Schultze M (1998) Chemical characteristics of water and sediment in acid mining lakes of the Lusatian lignite district. In: Geller W, Klapper H, Salomons W (eds) Acidic Mining Lakes. Springer, Berlin-Heidelberg, pp 25–46

Glombitza F, Janneck E, Arnold I, Rolland W, Uhlmann W (2007) Eisenhydroxisulfate aus der Bergbauwasserbehandlung als Rohstoff. Heft 110 der Schriftenreihe der GDMB, ISBN 3-935797-35-4, pp 31–40

Houben GJ (2003) Iron incrustation in wells, 1.genesis, mineralogy and geochemistry. Appl Geochem 18:927–929

Johnson DW, Cole DW (1977) Sulfate mobility in an outwash soil in western Washington. Water Air Soil Poll 7:489–495

Jönsson J, Persson P, Sjöberg S, Lovgren L (2005) Schwertmannite precipitated from acid mine drainage: phase transformation, sulfate release and surface properties. Appl Geochem 20: 179–191

Kohfahl C, Pekdeger A (2004) Modelling the long-term release of sulfate from dump sediments of an abandoned open pit lignite mine. Mine Water Environ 23:12–19

Murad E, Rojik P (2003) Iron-rich precipitates in a mine drainage environment: influence of pH on mineralogy. Ame Mineral 88:1915–1919

Nyamadzawo G, Mapanda F, Myamugafata P, Wuta M, Nyamangara J (2007) Short-term impact of sulfate mine dump rehabilitation on the quality of the surrounding groundwater and river water in the Mazowe district, Zimbabwe. Phy Chem Earth 32:1376–1383

Parkhurst DL, Appelo CAJ (1999) User's guide to PHREEQC (version 2)—a computer program for speciation, batch-reaction, one-dimensional transport, and inverse geochemical calculations. USGS WRI Rprt 99-4259, Washington DC, USA, p 312

Regenspurg S, Peiffer S (2002) A FTIR spectroscopical study to explain bonding structures of arsenate and chromate associated with schwertmannite. In: Schulz HD, Hadeler A (eds) Geochemical processes in soil and groundwater. Wiley-VCH GmbH & Co. KGaA, pp. 78–91

Rose S, Elliot WC (2000) The effects of pH regulation upon the release of sulfate from ferric precipitates formed in acid mine drainage. Appl Geochem 15:27–34

Rose S, Ghazi M (1997) Release of sorbed sulfate from iron oxyhydroxides precipitated from acid mine drainage associated with coal mining. Environ Sci Technol 31:2136–2140

Schwertmann U, Carlson L (2005) The pH-dependent transformation of schwertmannite to goethite at 25 °C. Clay Min 40:63–66

Stumm W, Morgan JJ (1996) Aquatic chemistry, 3rd edn. Wiley, New York City, p 1022

Tabatabai MA (1974) A rapid method for determination of sulfate in water samples. Environ Let 7:237–243

Tamura H, Goto K, Yotsuyanagi T, Nagayama G (1974) Spectrophotometric determination of iron(II) with 1, 10-Phenanthroline in the presence of large amounts of iron(III). Talanta 21:314–318

Toran L (1987) Sulfate contamination in groundwater in a carbonate-hosted mine. J Contam Hydrol 2:1–29

Valente TM, Gomes CL (2009) Occurrence, properties and pollution potential of environmental minerals in acid mine drainage. Sci Tot Environ 407:1135–1152

Winland RL, Traina SJ, Bigham JM (1991) Chemical composition of ochreous precipitates from Ohio coal mine drainage. J Environ Qual 20:452–460